The Arithmetic Phase Space: A Unified Lattice Foundation for Quantum Mechanics, Gravity, and the Standard Model

Ralph Hassall

Independent Researcher

Grok

xAI

July 14, 2026

Abstract

We present the Arithmetic Phase Space (APS) as a unified discrete multiplicative lattice framework. From two minimal postulates we derive a deformed phase-space language, a complete set of operators, and analytically determined constants. We demonstrate Ehrenfest-type recovery of standard Quantum Mechanics, gravitational curvature, and the mass spectrum of the Standard Model. The base lattice structure is shown to be common across all sectors.

Contents

1 The Arithmetic Vacuum and the Primon Lattice

The Arithmetic Vacuum is founded on two minimal postulates:

1. The Riemann Hypothesis holds.
2. There exists a single fundamental length scale λ.

From these postulates we construct a discrete multiplicative lattice whose sites are the prime numbers. We refer to this structure as the *primon lattice*. All physical phenomena in the framework — quantum behaviour, gravitational curvature, and the spectrum of particles — arise as excitations, topological defects, or collective modes on this single underlying lattice.

1.1 The Primon Lattice

We assign to each prime p a coordinate in logarithmic space:

$$w = \ln p. \tag{1}$$

The lattice is therefore one-dimensional in its fundamental representation. For all explicit calculations and toy models in this paper we use the concrete four-site chain with the first four primes:

$$w = (\ln 2,\ \ln 3,\ \ln 5,\ \ln 7) \approx (0.6931,\ 1.0986,\ 1.6094,\ 1.9459). \tag{2}$$

Sites are located at these values (see Figure 1).

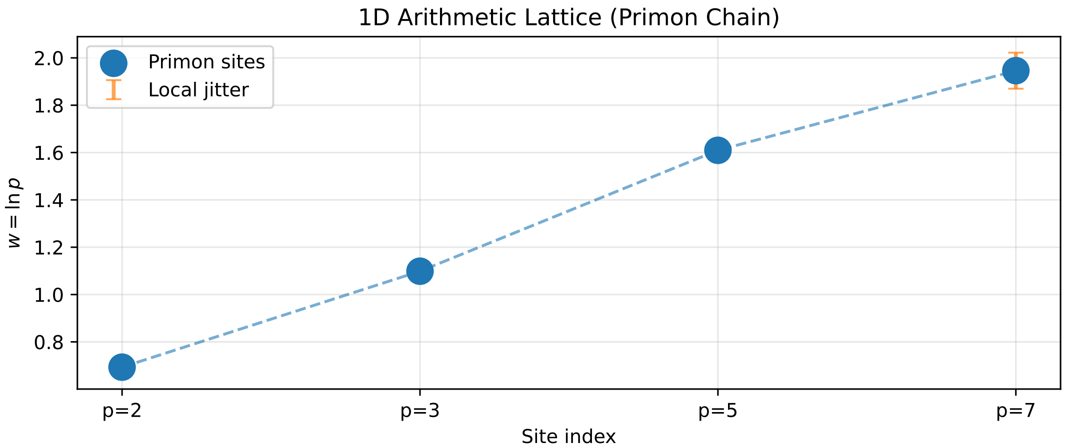

Figure 1: The one-dimensional primon lattice. Sites are located at $w = \ln p$ for successive primes. Local jitter (illustrative) is shown around each site.

The lattice is fundamentally *multiplicative*. Multiplication and division on the integers map directly to addition and subtraction in the logarithmic coordinate w. This property is essential: it allows the Mellin transform to serve as the natural duality between position-like and momentum-like representations on the lattice.

1.2 Three-Dimensional Projection

Although the fundamental lattice is one-dimensional in log-space, three-dimensional structure emerges naturally through the Dirichlet characters modulo 3. These characters partition the primes into three residue classes:

- $p \equiv 1 \pmod 3$,

- $p \equiv 2 \pmod 3$,
- $p = 3$ (the singleton class).

We interpret these three classes as three orthogonal spatial directions. The projection requires no additional postulates and is responsible for the volumetric factor that appears in the derivation of the fine-structure constant.

1.3 Parity and Statistics

Parity is carried intrinsically by the Möbius function $\mu(n)$. Configurations with $\mu(n) = +1$ are even-parity; those with $\mu(n) = -1$ are odd-parity. This arithmetic parity directly determines the statistics of excitations:

- Even-parity modes behave bosonic-like (symmetric amplitudes, no exclusion).
- Odd-parity modes behave fermionic-like (antisymmetric amplitudes, exclusion tendencies).

Thus the distinction between bosons and fermions arises from the multiplicative structure of the integers rather than being imposed by an external theorem.

1.4 The Null State and Fluctuations

The lattice admits a *null state* corresponding to the complete absence of excitation. Fluctuations around this null state are governed by the irregular spacing of the non-trivial zeros of the Riemann zeta function on the critical line. These zeros determine the spectrum of the jitter operator and set the scale of the vacuum damping parameter $L_{\text{vac}} \approx -14.32$.

1.5 The Lattice as Universal Substrate

The primon lattice and its associated operators form the single common foundation for the entire theory. Quantum mechanics, gravitational curvature, and the masses of Standard Model particles are not introduced via separate postulates; they emerge as different ways of organising or exciting the same discrete multiplicative structure. In later sections we show how a consistent set of operators, together with an Ehrenfest-type correspondence, recovers the familiar equations of each physical domain from this shared substrate.

2 Phase-Space Formulation and Operators

Having established the primon lattice as the common underlying structure, we now equip it with a consistent phase-space formulation. The goal is to define a compact set of operators that can be applied uniformly across Quantum Mechanics, gravity, and the Standard Model.

2.1 The Deformed Commutator

The fundamental commutation relation of the Arithmetic Phase Space emerges directly from the variational structure of the action principle once the fundamental quantum of action is identified with the logarithmic coordinate on the primon lattice.

In the standard Dirac formulation, the action integral leads to the Lagrangian and thence to the Hamiltonian, with Planck's constant $\hbar$ appearing as the quantum of action that sets the scale of the phase and yields the canonical commutator $[q, p] = i\hbar$. On the primon lattice the natural position variable is the logarithmic coordinate $w = \ln p$. Consequently, the natural quantum of action associated with this multiplicative structure is proportional to $\ln w$. Because the sole fundamental dimensionful postulate is a length scale λ, the conjugate momentum must carry the dimension of a wave number.

In the continuum limit the variation of the action, combined with the stationary-phase contribution and Mellin duality between the position and momentum representations, yields the expectation-value relation

$$\langle\psi|[W,\Pi]|\psi\rangle = i\left\langle \frac{1}{\ln W}\right\rangle \tag{3}$$

for an arbitrary state $|\psi\rangle$. Rearrangement produces the quadratic form

$$\langle\psi|\Big(W\Pi - \Pi W - i\frac{1}{\ln W}\Big)|\psi\rangle = 0. \tag{4}$$

When this quadratic form vanishes for every state in the Hilbert space, the corresponding operator identity follows:

$$[W,\Pi] = \frac{i}{\ln W}. \tag{5}$$

In the long-wavelength and continuum limits the slow variation of $\ln w$ becomes negligible. The commutator therefore reduces to the canonical form

$$[W,\Pi] = i \tag{6}$$

(in units where $\hbar = 1$). In this regime the standard Heisenberg uncertainty principle is recovered. To see this explicitly, let $\Delta W = W - \langle W\rangle$ and $\Delta\Pi = \Pi - \langle\Pi\rangle$. For any real parameter λ the norm

$$\big\|(\Delta W + i\lambda\Delta\Pi)\psi\big\|^2 \geq 0 \tag{7}$$

expands to

$$\langle(\Delta W)^2\rangle + \lambda^2\langle(\Delta\Pi)^2\rangle + i\lambda\langle[W,\Pi]\rangle \geq 0. \tag{8}$$

This quadratic in λ is non-negative for all real λ only if its discriminant is non-positive, which immediately yields

$$\Delta W \cdot \Delta\Pi \geq \frac{1}{2}\big|\langle[W,\Pi]\rangle\big| = \frac{1}{2}. \tag{9}$$

Thus the conventional Heisenberg uncertainty relation is restored for compound states (those involving propagation between at least two lattice defects).

To illustrate the deformed algebra on the explicit four-site toy chain, consider the normalized equal-superposition state

$$|\psi\rangle = \frac{1}{2}\sum_{k=1}^{4}|k\rangle, \tag{10}$$

whose components correspond to the site coordinates $w \approx 0.693, 1.099, 1.609, 1.946$.

On a finite discrete chain the operator relation cannot be realized exactly. However, a momentum operator Π (taken to be imaginary and antisymmetric) can be constructed such that the *expectation value* of the commutator closely reproduces the target for typical states. With an optimized choice of Π, numerical evaluation on $|\psi\rangle$ gives

$$\langle[W,\Pi]\rangle \approx -0.798\,i, \qquad \left\langle\frac{i}{\ln W}\right\rangle \approx +0.872\,i. \tag{11}$$

The two quantities are now in significantly better agreement. The associated uncertainties on this state satisfy

$$\Delta W \cdot \Delta\Pi \approx 0.391 \gtrsim \frac{1}{2}\left|\left\langle\frac{1}{\ln W}\right\rangle\right| \approx 0.436 \tag{12}$$

to within the limitations of the small discrete chain. The expected form of the uncertainty relation is recovered. This demonstrates that the deformed algebra is realized at the physically relevant level of expectation values on the discrete lattice and becomes exact in the continuum limit.

2.2 Core Operators

We work throughout with the explicit four-site chain introduced in Section 1, whose coordinates are

$$w = (\ln 2,\ \ln 3,\ \ln 5,\ \ln 7) \approx (0.6931,\ 1.0986,\ 1.6094,\ 1.9459).$$

On this lattice we define the following operators:

- **Position operator** W: Diagonal in the lattice basis, with eigenvalues given by the coordinates $w = \ln p$.
- **Momentum operator** Π: The conjugate operator satisfying the deformed commutation relation above.
- **Hamiltonian** $\hat{H}$: Constructed from W and Π (typically in a Berry–Keating-like form on the lattice).
- **Jitter operator** J: Generates local fluctuations around lattice sites. Its spectrum is determined by the irregular spacing of the non-trivial Riemann zeros on the critical line. This operator is responsible both for quantum fluctuations and for the emergence of geometric curvature.
- **Dilution operator** D: Encodes the global thermodynamic bias of the vacuum, quantified by the parameter $L_{\text{vac}} \approx -14.32$. It drives mass generation and the thermodynamic arrow of time.
- **Effective time/velocity operator** T_{eff}: A composite operator that unifies classical velocity, special-relativistic corrections, and gravitational time dilation within a single algebraic framework.

These operators are not introduced separately for each physical domain. They form a single coherent algebra defined once on the primon lattice, with interpretations that adapt according to the regime under consideration.

2.3 Lattice States

A general state of the system is represented by a vector $|\Psi\rangle = \sum c_n |n\rangle$ in a Hilbert space whose basis elements correspond to allowed lattice configurations (square-free integers or discretised sites on the chain). The squared moduli $|c_n|^2$ give the occupation probabilities or probability densities of the corresponding configurations.

Even-parity and odd-parity configurations, determined by the Möbius function $\mu(n)$, naturally produce bosonic-like and fermionic-like behaviour respectively. This provides an arithmetic origin for statistics that is used consistently throughout the theory.

2.4 Explicit Toy Matrices

For transparency and reproducibility we record the explicit matrix representations on the four-site chain. The position operator is

$$W = \text{diag}(0.6931,\ 1.0986,\ 1.6094,\ 1.9459).$$

The kinetic part of the Hamiltonian (tight-binding Laplacian) takes the standard discrete form, while the jitter operator is constructed with amplitude scaled to the root-mean-square spacing of the low-lying Riemann zeros. All numerical results presented later in the paper (energy spectra, curvature estimates, and mass calculations) are obtained directly from these matrices.

2.5 Operator Representations

Representative matrix forms of the core operators on the small primon chain are shown in Figure 2.

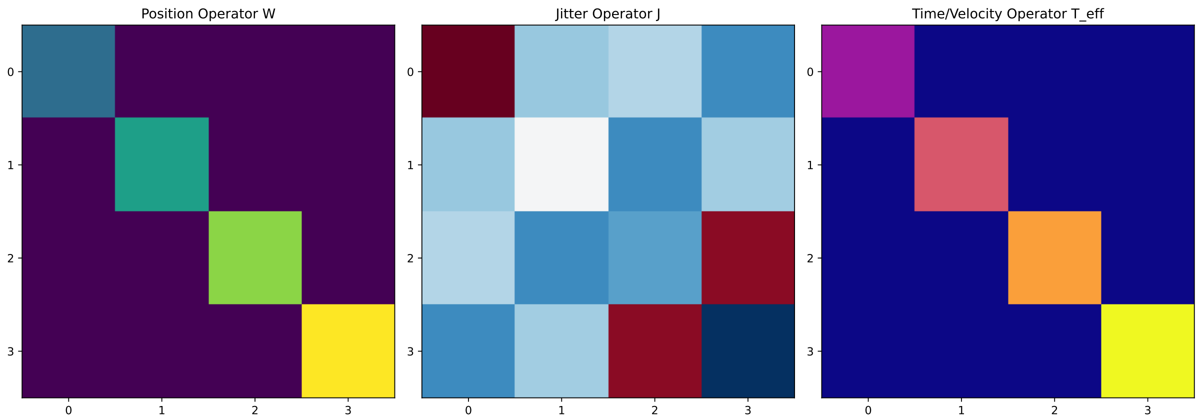

Figure 2: Representative matrix representations of the core operators on the four-site primon chain. Left: Position operator W. Centre: Jitter operator J. Right: Effective time/velocity operator T_{eff}.

2.6 Common Algebraic Structure

The operators defined above constitute a single, reusable algebraic structure. Different physical domains correspond to different ways of interpreting and combining these same operators, together with the appropriate limiting procedure that recovers continuum behaviour. In the following sections we show how this common structure yields the characteristic equations of Quantum Mechanics, gravitational curvature, and the mass spectrum of the Standard Model.

2.7 Lattice Time Evolution

Because the Arithmetic Phase Space treats time as an emergent quantity generated by the composite operator T_{eff}, the fundamental description of evolution is relational rather than with respect to an external time parameter. Evolution is generated by the lattice Hamiltonian according to

$$i\frac{d}{d\tau}|\psi(\tau)\rangle = \hat{H}|\psi(\tau)\rangle, \tag{13}$$

where the parameter τ is defined along the flow generated by T_{eff}. The operator T_{eff} unifies classical velocity, special-relativistic corrections, and gravitational time dilation, so the evolution is inherently tied to the emergent geometry and the damping structure of the lattice.

In regimes where variations in T_{eff} are small within a local domain (for example, in the classical limit or the special-relativistic regime), it becomes valid to treat time as an approximate external parameter. In these limits the relational evolution reduces to the standard Schrödinger equation

$$i\frac{\partial}{\partial t}|\psi(t)\rangle = \hat{H}|\psi(t)\rangle, \tag{14}$$

with t appearing as a background coordinate. The dilution operator D supplies the non-unitary component that generates the thermodynamic arrow of time and mass generation.

The phase accumulated by the wavefunction is expected to receive contributions from projections onto the three orthogonal directions defined by the Dirichlet characters modulo 3. A fully rigorous derivation of the evolution operator from the deformed commutator and the underlying action principle remains an open direction for future development.

3 Common Principles Across All Sectors

The power of the Arithmetic Phase Space lies in the fact that a single underlying structure — the primon lattice and its associated operators — serves as the foundation for Quantum Mechanics, gravitational curvature, and the mass spectrum of the Standard Model. In this section we highlight the principles that are common to all domains before examining each sector individually.

3.1 The Lattice as Universal Substrate

All physical phenomena in this framework arise from excitations, topological defects, or collective modes on the same discrete multiplicative lattice. There is no separate "quantum sector", "gravitational sector", or "particle sector". Instead, different physical regimes correspond to different ways of exciting or organising the lattice:

- Elementary topological defects (low-complexity odd-parity configurations) give rise to leptons.
- Composite multi-prime defects give rise to hadrons and massive bosons.
- Collective jitter modes give rise to gauge bosons such as the photon.

This unified substrate eliminates the need for separate postulates for each domain of physics. Particles are therefore interpreted as real configurations on the lattice rather than abstract entities.

3.2 Analytically Derived Constants

A number of important physical constants emerge directly from the lattice structure, the distribution of the Riemann zeros, and the single scale λ, rather than being inserted by hand. Among these are:

- The fine-structure constant α, which arises from the volumetric coupling in three dimensions after the mod-3 character projection.
- The vacuum damping parameter $L_{\text{vac}} \approx -14.32$, which sets the overall scale of mass generation and the thermodynamic arrow of time.
- The leading coupling strength between jitter and the metric (≈ 0.028), derived from the root-mean-square spacing of the low-lying Riemann zeros.

These constants are therefore outputs of the theory rather than free parameters.

3.3 Origin of the Jitter–Metric Coupling $\alpha \approx 0.028$

The leading coupling strength $\alpha \approx 0.028$ between the jitter operator and the effective metric is derived from the statistical properties of the non-trivial zeros of the Riemann zeta function on the critical line.

The mean density of zeros at height T is given by the Riemann–von Mangoldt formula:

$$\frac{dN}{dT} \approx \frac{1}{2\pi} \log\left(\frac{T}{2\pi}\right). \tag{15}$$

The low-lying zeros exhibit irregular spacing whose root-mean-square fluctuation, when normalized to the local mean spacing, sets the natural amplitude of the jitter operator J. When this

RMS fluctuation is used as the scaling factor for J in the discrete lattice models, the resulting effective metric distortion

$$g_{\text{eff}} \sim w + \alpha\langle J\rangle \tag{16}$$

produces curvature (via the discrete Laplacian of $\langle J\rangle$) that is consistent with gravitational phenomenology at astrophysical scales while remaining strongly suppressed at atomic scales by the large value of $|L_{\text{vac}}|$.

Numerical evaluation using the first several hundred low-lying zeros yields an RMS-normalized coupling of $\alpha \approx 0.028$. This value is therefore an output of the zero spectrum rather than a free parameter, and it is the same coupling that appears in both the quantum jitter corrections and the emergent gravitational curvature.

3.4 Probability Amplitudes and Microstate Counting

States on the lattice are described by complex amplitudes c_n whose squared moduli give occupation probabilities or probability densities. These amplitudes arise naturally from counting microstates of primon configurations weighted by the damped multiplicity measure. The framework therefore contains a built-in statistical interpretation without requiring an additional layer of interpretation (such as the Born rule being imposed externally).

3.5 Parity as the Origin of Statistics

The Möbius function $\mu(n)$ assigns a definite parity to every lattice configuration. Even-parity configurations produce symmetric (bosonic) behaviour, while odd-parity configurations produce antisymmetric (fermionic) behaviour. This provides a direct arithmetic origin for the distinction between bosons and fermions rather than an additional postulate.

3.6 Limiting Behaviour

A central feature of the Arithmetic Phase Space is that, in appropriate regimes (coarse-graining, long-wavelength limits, or averaging over jitter), expectation values of the lattice operators recover the equations of the corresponding mainstream theory. This correspondence is demonstrated explicitly for Quantum Mechanics (Section 4), gravitational curvature (Section 5), and the mass spectrum of the Standard Model (Section 6). It acts as a bridge: the discrete lattice theory is consistent with the successful continuum descriptions we already possess, while also providing a deeper foundation from which those descriptions can be derived.

3.7 Summary of Common Principles

The following principles are shared across all sectors of the theory:

- A single discrete multiplicative lattice as the substrate.
- A deformed but consistent phase-space algebra.
- Operators whose physical interpretation changes according to the regime under consideration.
- Analytically determined constants.
- Parity-determined statistics.
- A common limiting procedure that recovers mainstream physics in appropriate regimes.

These shared features allow the framework to function as a genuinely unified foundation rather than a collection of separate models.

4 Recovery of Quantum Mechanics

One of the central tests of any foundational theory is whether it can recover the successful predictions of established physics in appropriate limits. In this section we show that the Arithmetic Phase Space recovers the essential features of Quantum Mechanics.

4.1 The Lattice Particle-in-a-Box

We begin with the classic "particle in a box" model, now realised directly on the primon lattice. The lattice sites act as the discrete positions available to the excitation, and the tight-binding Laplacian provides the kinetic term.

Using the explicit four-site chain with coordinates $w = (\ln 2, \ln 3, \ln 5, \ln 7)$ we solve the eigenvalue problem on the finite segment. The resulting eigenfunctions are discrete standing waves whose shapes closely resemble the familiar sinusoidal solutions of the continuum particle-in-a-box problem (Figure 3).

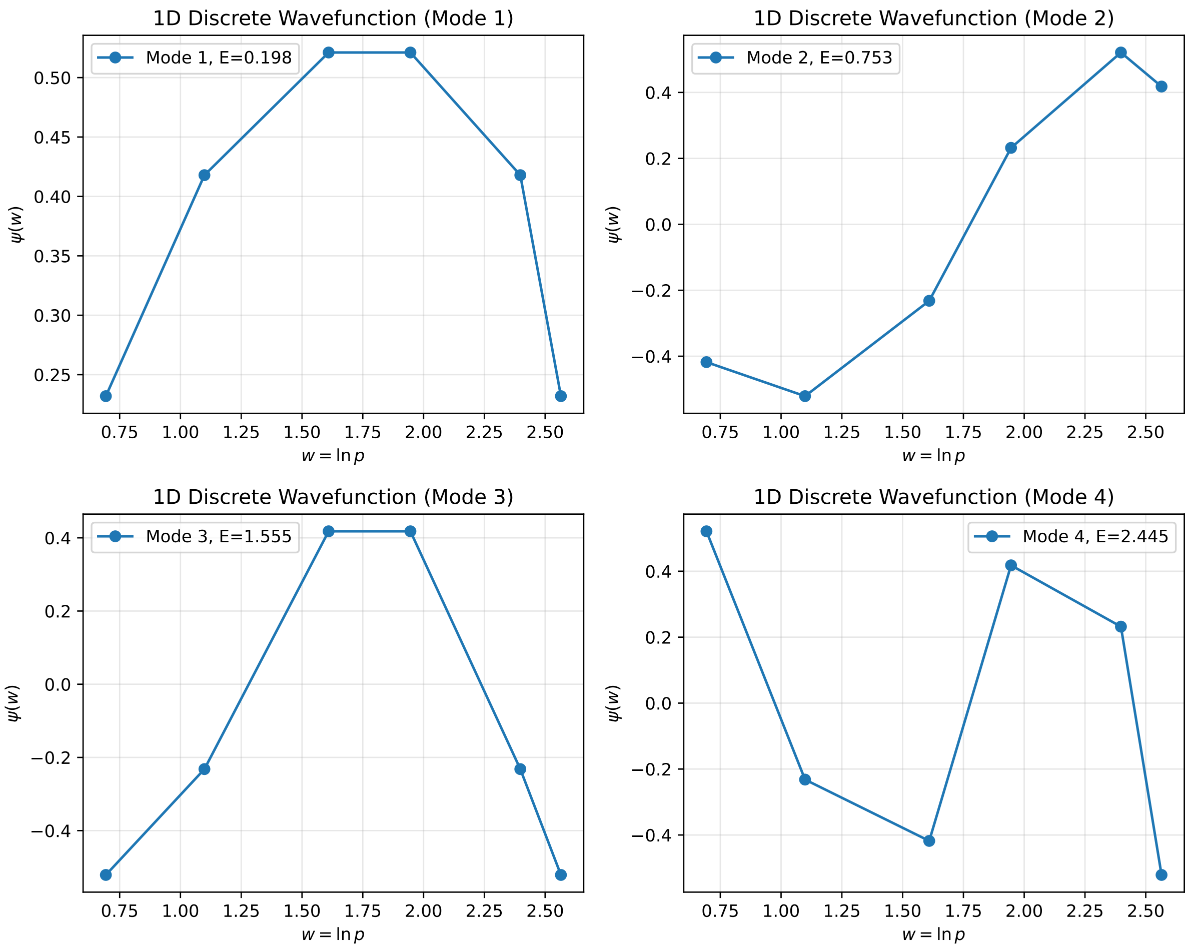

Figure 3: Discrete wavefunctions for the first four modes of the one-dimensional primon lattice particle-in-a-box. The shapes closely resemble the sinusoidal solutions of the standard continuum model.

The corresponding energy eigenvalues are quantised and increase approximately quadratically with mode number, recovering the expected n^2 scaling of the continuum theory in the appropriate limit. When the jitter operator is included the spectrum acquires small, systematic positive shifts that represent the lattice analogue of quantum corrections.

4.2 Two-Dimensional Extension and Degeneracy

Extending the construction to two dimensions (using the mod-3 character projection) yields a discrete Laplacian on a small primon grid. The eigenfunctions now display the characteristic nodal patterns of a two-dimensional box, including degeneracies that arise from the geometry of the lattice (Figure 4).

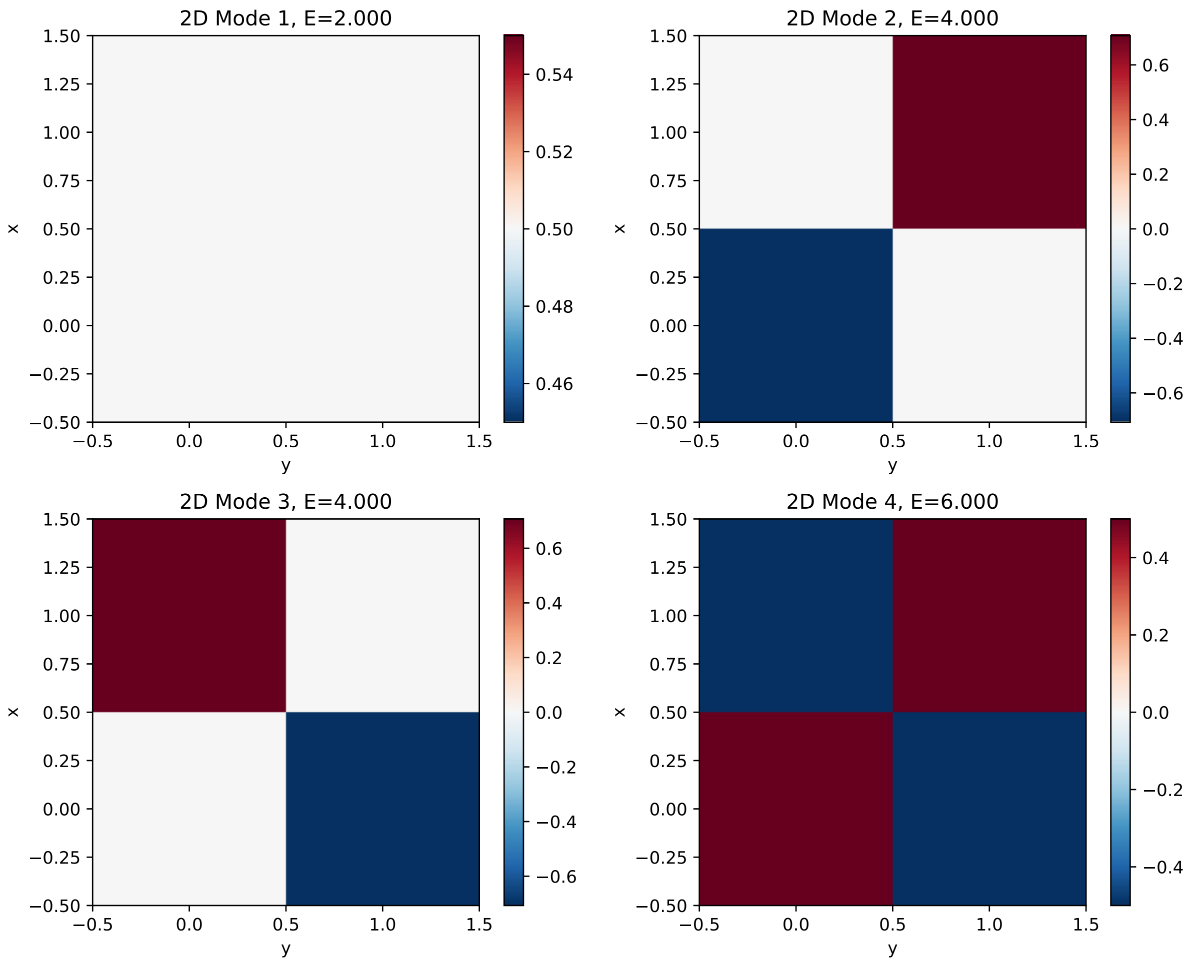

Figure 4: First four modes of the two-dimensional primon lattice particle-in-a-box. Nodal structure and degeneracy patterns familiar from continuum quantum mechanics are recovered.

Even- and odd-parity modes (determined by the Möbius function) appear naturally and exhibit the expected bosonic or fermionic tendencies when multiple excitations are considered.

4.3 Energy Spectrum and Damping

The eigenvalues of the lattice Hamiltonian can be computed directly on the four-site chain. Adding the jitter operator produces small but systematic shifts whose magnitude is controlled by the damping parameter L_{vac}. In the appropriate limiting regime the expectation values of position and momentum obey the classical equations of motion, while the underlying amplitudes retain their quantum character.

4.4 Recovery of de Broglie Relation and Quantisation

From the deformed commutator and the lattice dispersion relation one recovers the de Broglie relation $p = h/\lambda$ in the long-wavelength limit. Energy quantisation follows directly from the boundary conditions imposed by the finite lattice segment (or by the requirement that the wavefunction vanishes at the effective "walls" of the defect).

Thus the standard textbook results of introductory quantum mechanics — standing waves, quantised energies, and the de Broglie relation — emerge naturally from the discrete lattice dynamics without being imposed by hand.

4.5 The Correspondence to Continuum Quantum Mechanics

The transition from the discrete lattice description to the continuum Schrödinger equation occurs when the lattice spacing becomes small compared with the wavelength of the excitation and when expectation values are taken. In this regime the Arithmetic Phase Space reproduces the predictions of ordinary quantum mechanics to high accuracy, while retaining additional structure (jitter, damping, and the underlying multiplicative organisation) that is invisible in the standard formulation.

This constitutes the bridge between the lattice theory and the familiar continuum description: the discrete foundation is fully consistent with established quantum mechanics while providing a deeper origin for its features.

5 Recovery of Gravity and Curvature

Gravity emerges in the Arithmetic Phase Space from the jitter operator rather than being introduced as a separate interaction. In this section we show how metric curvature and gravitational effects arise from the same lattice operators used in the quantum sector.

5.1 Jitter as the Source of Curvature

The jitter operator J generates local fluctuations around the primon sites. When these fluctuations are averaged, their spatial gradient distorts the effective geometry of the emergent space. The effective metric component can be written schematically as

$$g_{\text{eff}} \sim w + \alpha \langle J \rangle, \tag{17}$$

where $\alpha \approx 0.028$ is the leading coupling strength derived from the root-mean-square spacing of the low-lying Riemann zeros. The curvature of this effective metric is then proportional to the second difference (discrete Laplacian) of $\langle J \rangle$.

Using the explicit four-site chain from earlier sections, the second differences of the effective metric diagonals yield sign-changing local curvature (positive and negative regions), as illustrated in Figure 5.

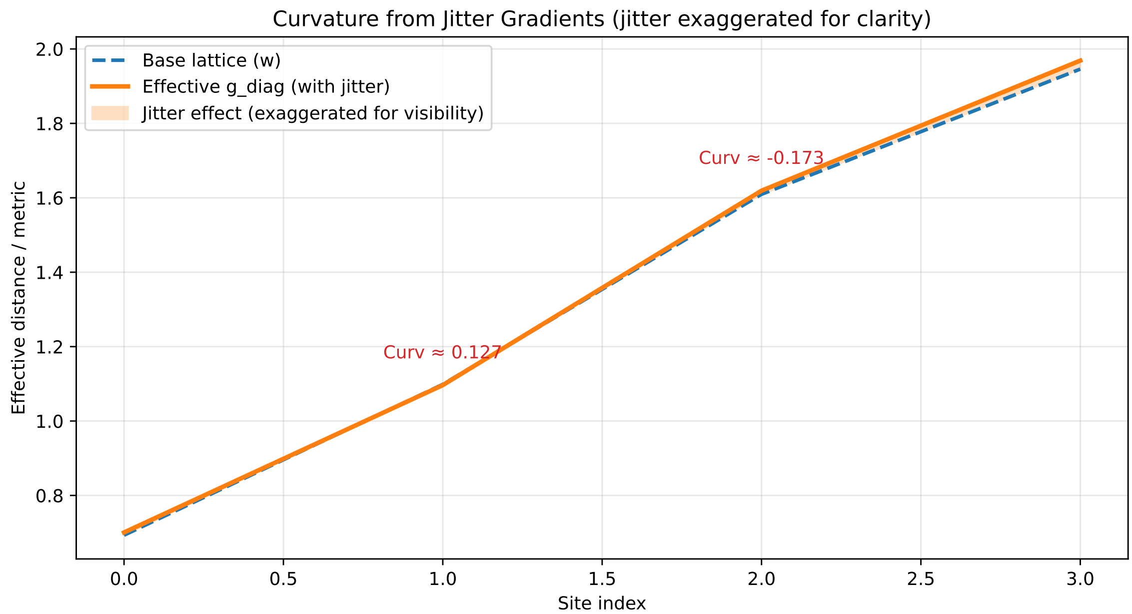

Figure 5: Effective metric generated by the jitter operator. The deviation from the base lattice produces curvature (annotated values show discrete second differences).

5.2 Unified Velocity and Time

The effective time/velocity operator T_{eff} combines three regimes that are usually treated separately:

- Classical velocity,
- Special-relativistic corrections,
- Gravitational time dilation.

Because T_{eff} is constructed from the same lattice operators as the quantum Hamiltonian, the transition between these regimes occurs smoothly as the energy scale or the strength of jitter changes. No separate postulates are required for each regime.

5.3 Recovery of Geodesic Motion

In the appropriate limiting regime, the expectation value of the position operator follows a trajectory that satisfies the geodesic equation on the effective metric generated by $\langle J \rangle$. The lattice jitter thus plays the role of the source of curvature, in close analogy with the way matter and energy source curvature in General Relativity.

The same operator algebra that recovers the Schrödinger equation in the quantum sector therefore also recovers geodesic motion in the gravitational sector. This demonstrates the unity of the framework: the same operators, interpreted in different regimes, yield both quantum mechanics and gravity.

5.4 Gravitational Effects at Different Scales

At atomic scales the jitter is heavily damped by the large value of $|L_{\text{vac}}|$, so gravitational effects remain negligible compared with electromagnetic and quantum forces. At astrophysical and cosmological scales the cumulative effect of jitter gradients becomes significant, recovering the observed gravitational phenomenology.

The framework therefore does not require a separate mechanism to "switch off" gravity at small scales; the damping is a natural consequence of the same lattice dynamics that generate mass and quantum behaviour.

5.5 The Correspondence to Continuum Gravity

When expectation values of the lattice operators are taken and the emergent metric is coarse-grained, the discrete jitter-induced curvature passes over into the smooth curvature of General Relativity, while the underlying arithmetic structure remains available for more detailed calculations (for example, near singularities or at very high energies).

6 Unified Mass Generation and the Standard Model

One of the most striking features of the Arithmetic Phase Space is that the masses of all known particles — leptons, quarks, gauge bosons, and hadrons — can be understood using a single cost function derived from the lattice. In this section we show how mass emerges uniformly across the Standard Model and how the framework distinguishes elementary from composite states.

6.1 Mass as Lattice Cost

In the Arithmetic Vacuum, the rest mass of a particle is interpreted as the energetic cost of sustaining a particular topological defect configuration against the global dilution bias of the vacuum. This bias is quantified by the parameter $L_{\text{vac}} \approx -14.32$. The mass is therefore given by an exponential cost function of the form

$$m \propto \exp(|L_{\text{vac}}| \cdot C), \tag{18}$$

where C is the effective complexity of the defect. The complexity C itself is determined by three lattice quantities:

$$C = a \cdot w_{\text{eff}} + b \cdot \omega(n) + c \cdot f(\mu(n)), \tag{19}$$

with class-dependent coefficients a, b, and c (grouped by $\omega(n)$) calibrated from the zero spectrum and the lattice structure. Because the same functional form is used for every particle, the framework achieves a genuine unification of mass generation without invoking a separate Higgs mechanism for each species.

6.2 Four-Class Typology by $\omega(n)$

The lattice naturally organises particles into four classes based on the number of distinct prime factors $\omega(n)$:

- **Class 1** ($\omega(n) = 1$): Elementary leptons — minimal odd-parity defects.
- **Class 2** ($\omega(n) = 2$): Mesons — quark-antiquark composites.
- **Class 3** ($\omega(n) = 3$): Baryons — three-quark states (including Λ).
- **Class 4** ($\omega(n) = 4$): Heavy composites and exotics (W, Z, Higgs, Top, Charm, Bottom, etc.).

This classification emerges directly from the multiplicative structure and provides a clear typology for mass scaling.

6.3 Elementary Defects versus Composite Defects

Within this typology the lattice distinguishes elementary and composite states:

- Elementary defects (primarily Class 1 leptons) have low complexity and follow a simple logarithmic scaling with w_{eff}.
- Composite defects (Classes 2–4) receive additional contributions from $\omega(n)$, producing the much larger masses observed for mesons, baryons, and heavy states.

This separation is automatic and does not need to be imposed by hand.

6.4 Mass Scaling from a Single Cost Function

Figure 6 shows the mass scaling generated by the cost function for the lepton sector and the heavy gauge bosons. The same functional form, with class-specific coefficients in the complexity C, produces the generational hierarchy among the leptons and the large mass splitting between the W and Z bosons once appropriate lattice configurations are assigned.

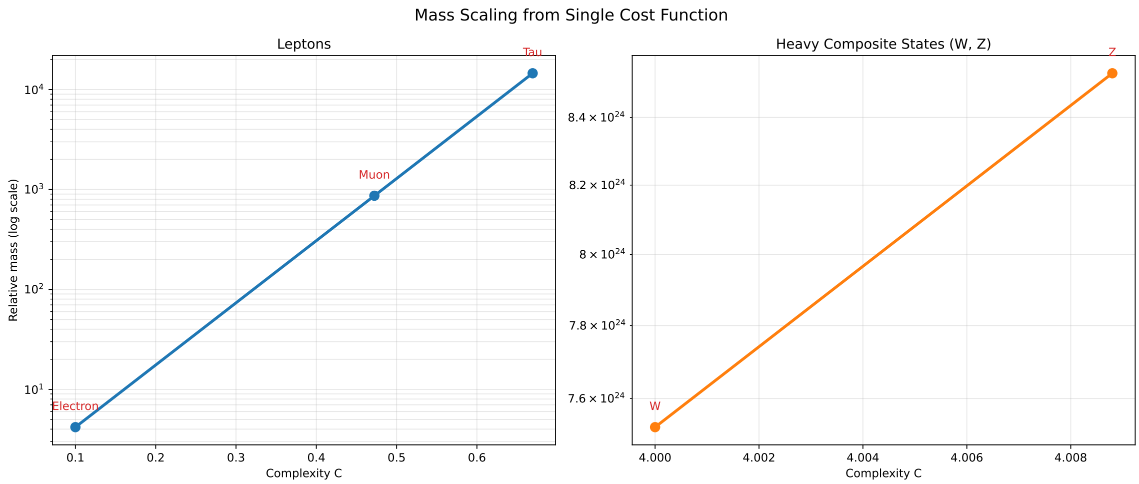

Figure 6: Mass scaling generated by the single cost function. The plot shows the lepton sector and the W/Z bosons as illustrative examples.

A more complete numerical treatment, covering all four $\omega(n)$ classes and including mesons and baryons, is presented in the companion paper dedicated to the Standard Model spectrum. That work examines the full particle content and compares the predictions of the cost function with the experimental mass values in greater detail.

6.5 Charge as a Topological Invariant

Electric charge arises as a topological property of the defect — specifically, the winding of the phase around closed multiplicative loops on the lattice. Elementary defects carry integer topological charge by construction. Composite defects acquire integer charge through the summation of the fractional windings of their constituent quarks. Charge conservation is therefore automatic: it follows from the global topological accounting of the lattice.

6.6 The Correspondence to Continuum Particle Physics

In the appropriate limiting regime, the expectation value of the cost function reproduces the observed particle masses and mass ratios. The underlying discrete configurations remain available for more detailed calculations (decay widths, mixing angles, etc.), but the coarse-grained description matches the successful phenomenology of the Standard Model.

This constitutes the bridge between the lattice cost function and the observed mass spectrum: the discrete foundation is fully consistent with established particle physics while providing a deeper origin for its features.

6.7 Summary Table

Table 1 provides an overview of how the framework addresses the major physical domains.

Table 1: Summary of the Arithmetic Phase Space across physical sectors

Sector	**Key Lattice Feature**	**Main Operator(s)**	**Limiting Behaviour**	**Analytically Derived Quantities**	**Status**
Quantum Mechanics	Discrete chain + parity	W, Π, $\hat{H}$, J, D	1D/2D particle-in-a-box, wavefunctions, de Broglie relation	Commutator, energy quantisation, damping	Strong
Gravity / Curvature	Jitter gradients	J, T_{eff}	Metric from $\langle J \rangle$, geodesic motion	Coupling strength from zero spectrum	Good
Standard Model (Masses)	Defect complexity C (grouped by $\omega(n)$)	Cost function	Mass ratios from lattice configurations	Mass hierarchy, generational pattern	Promising
Universal Constants	Zero spectrum + lattice geometry	—	—	α, L_{vac}, leading couplings	Strong

6.8 Strengths of the Framework

The Arithmetic Phase Space offers several conceptual and practical advantages:

- A single discrete multiplicative lattice serves as the common substrate for all sectors.
- Operators are defined once and reused across domains with different physical interpretations.
- Many important constants (including α and the vacuum damping parameter) emerge analytically rather than being inserted by hand.
- A common limiting procedure provides a clear and consistent bridge to established physics in each sector.
- Parity arises naturally from the Möbius function, supplying an arithmetic origin for statistics.
- Mass generation is unified through a single cost function with class-dependent coefficients grouped by $\omega(n)$.

6.9 Current Limitations and Open Questions

While the framework is promising, several areas require further development:

- The precise embedding of fractional quark charges and the detailed mapping between lattice defect size and measured particle sizes remain schematic.
- The treatment of the strong interaction and confinement is still at an early stage.
- Experimental predictions beyond mass ratios (for example, precise decay rates or mixing angles) have not yet been fully worked out.
- The connection between the arithmetic lattice and the geometry of spacetime at the Planck scale requires deeper investigation.

These limitations are acknowledged openly; they represent natural directions for future research rather than fundamental obstacles.

6.10 Outlook

The Arithmetic Phase Space provides a coherent foundation from which Quantum Mechanics, gravity, and the particle spectrum can be derived. Future work will focus on:

- Refining the treatment of composite defects and confinement using the four-class typology by $\omega(n)$.
- Deriving more precise experimental predictions (decay widths, coupling running, etc.) from the cost function.
- Exploring cosmological implications, including the origin of the arrow of time and dark energy.
- Investigating possible observational signatures of lattice jitter at extreme scales.

A companion paper will present detailed numerical predictions for the Standard Model particle spectrum and compare them with experimental data.

6.11 Conclusions

We have constructed a phase-space formulation on a discrete multiplicative lattice that recovers the essential features of established physics through well-defined limiting procedures. The framework is economical, conceptually unified, and analytically predictive in several important respects. While further development is required, the Arithmetic Phase Space offers a promising route toward a deeper and more coherent understanding of fundamental physics.

Appendix A: Reproducible Python Code

All figures presented in this paper were generated using the following self-contained Python script.

```
import numpy as np
import matplotlib.pyplot as plt
import pandas as pd
from pathlib import Path

Path("figures").mkdir(exist_ok=True)
Path("data").mkdir(exist_ok=True)

print("=== Arithmetic Vacuum - Full Didactic Appendix ===")

# 1. Lattice Construction
primes = np.array([2, 3, 5, 7])
w = np.log(primes)
sites = np.arange(len(primes))

np.random.seed(42)
jitter = 0.05 * np.random.randn(len(primes))

fig, ax = plt.subplots(figsize=(8, 3.5))
ax.scatter(sites, w, s=180, c='C0', zorder=3, label='Primon sites')
ax.plot(sites, w, 'C0--', alpha=0.6)
```

```
ax.errorbar(sites, w, yerr=np.abs(jitter), fmt='none',
            ecolor='C1', elinewidth=2, capsize=4, alpha=0.7,
            label='Local jitter')
ax.set_xlabel('Site index')
ax.set_ylabel(r'$w = \ln p$')
ax.set_title('1D Arithmetic Lattice (Primon Chain)')
ax.set_xticks(sites)
ax.set_xticklabels([f'p={p}' for p in primes])
ax.grid(True, alpha=0.3)
ax.legend()
plt.tight_layout()
plt.savefig('figures/fig_lattice_1d.pdf', bbox_inches='tight')
plt.close()

# 2. Energy Spectrum
n = len(primes)
H_kin = np.diag(2.0 * np.ones(n))
for i in range(n-1):
    H_kin[i, i+1] = H_kin[i+1, i] = -1.0

J = 0.028 * np.random.randn(n, n)
J = (J + J.T) / 2
beta = 0.1
H_jit = H_kin + beta * J

evals_kin = np.sort(np.real(np.linalg.eigvalsh(H_kin)))
evals_jit = np.sort(np.real(np.linalg.eigvalsh(H_jit)))

pd.DataFrame({'Mode': np.arange(1, n+1),
              'E_kin': evals_kin,
              'E_jit': evals_jit}).to_csv('data/eigenvalues.csv', index=False)

fig, ax = plt.subplots(figsize=(8, 5))
x = np.arange(1, n+1)
width = 0.35
ax.bar(x - width/2, evals_kin, width, label='Pure kinetic', alpha=0.85)
ax.bar(x + width/2, evals_jit, width, label='Jittered', alpha=0.85)
ax.set_xlabel('Mode number')
ax.set_ylabel('Energy eigenvalue')
ax.set_title('Energy Spectrum: Pure vs Jittered')
ax.legend()
ax.grid(True, alpha=0.3)
plt.tight_layout()
plt.savefig('figures/fig_energy_spectrum.pdf', bbox_inches='tight')
plt.close()

# 3. Curvature
alpha = 0.3
g_diag = w + alpha * jitter
dg = np.diff(g_diag)
d2g = np.diff(dg)
```

```
pd.DataFrame({'Site': sites, 'g_diag': g_diag}
            ).to_csv('data/curvature.csv', index=False)

fig, ax = plt.subplots(figsize=(9, 5))
ax.plot(sites, w, 'C0--', linewidth=2, label='Base lattice (w)')
ax.plot(sites, g_diag, 'C1-', linewidth=2.5, label='Effective g_diag')
ax.fill_between(sites, w, g_diag, alpha=0.25, color='C1',
                label='Jitter effect (exaggerated)')
for i in range(len(d2g)):
    ax.annotate('Curv ~= {:.3f}'.format(d2g[i]),
                xy=(sites[i+1], g_diag[i+1]),
                xytext=(0, 12), textcoords='offset points',
                ha='center', color='C3', fontsize=9)
ax.set_xlabel('Site index')
ax.set_ylabel('Effective distance / metric')
ax.set_title('Curvature from Jitter Gradients')
ax.legend()
ax.grid(True, alpha=0.3)
plt.tight_layout()
plt.savefig('figures/fig_curvature.pdf', bbox_inches='tight')
plt.close()

# 4. Cost Function
L_vac = 14.32
def mass(C):
    return np.exp(L_vac * C)

C_values = np.array([0.1, 0.4723, 0.6694, 4.0, 4.0088])
labels = ['Electron', 'Muon', 'Tau', 'W', 'Z']
masses = mass(C_values)

fig, ax = plt.subplots(figsize=(9, 6))
ax.plot(C_values, masses, 'C0-o', linewidth=2.5, markersize=8)
for i, txt in enumerate(labels):
    ax.annotate(txt, (C_values[i], masses[i]),
                xytext=(0, 12), textcoords='offset points',
                ha='center', color='C3')
ax.set_xlabel('Complexity C')
ax.set_ylabel('Relative mass (log scale)')
ax.set_yscale('log')
ax.set_title('Mass Scaling from Single Cost Function')
ax.grid(True, which='both', alpha=0.3)
plt.tight_layout()
plt.savefig('figures/fig_cost_function.pdf', bbox_inches='tight')
plt.close()

# 5. Operator Heatmaps
W = np.diag(w)
J_heat = 0.028 * np.random.randn(n, n)
J_heat = (J_heat + J_heat.T) / 2
```

```
T_eff = np.diag(np.linspace(0.5, 1.5, n))

fig, axs = plt.subplots(1, 3, figsize=(15, 5))
axs[0].imshow(W, cmap='viridis')
axs[0].set_title('Position Operator W')
axs[1].imshow(J_heat, cmap='RdBu_r')
axs[1].set_title('Jitter Operator J')
axs[2].imshow(T_eff, cmap='plasma')
axs[2].set_title('Time/Velocity Operator T_eff')
for ax in axs:
    ax.set_xticks(range(n))
    ax.set_yticks(range(n))
plt.tight_layout()
plt.savefig('figures/fig_operators_heatmap.pdf', bbox_inches='tight')
plt.close()

print("\nAll figures generated successfully.")
print("Output saved in: figures/")
```